Atmos. Meas. Tech. Discuss., 4, 5389–5424, 2011
www.atmos-meas-tech-discuss.net/4/5389/2011/
doi:10.5194/amtd-4-5389-2011

Atmospheric Measurement Techniques Discussions

Global distributions of C_2H_6, C_2H_2, HCN, and PAN retrieved from MIPAS reduced spectral resolution measurements

A. Wiegele, N. Glatthor, M. Höpfner, U. Grabowski, S. Kellmann, A. Linden, G. Stiller, and T. von Clarmann

Karlsruher Institut für Technologie, Institut für Meteorologie und Klimaforschung, Karlsruhe, Germany

Received: 29 July 2011 – Accepted: 10 August 2011 – Published: 19 August 2011

Correspondence to: A. Wiegele (andreas.wiegele@kit.edu)

Published by Copernicus Publications on behalf of the European Geosciences Union.

Abstract

Vertical profiles of mixing ratios of C_2H_6, C_2H_2, HCN, and PAN were retrieved from MIPAS reduced spectral resolution nominal mode limb emission measurements. The retrieval strategy followed that of the analysis of MIPAS high resolution measurements, with occasional adjustments to cope with the reduced spectral resolution under which MIPAS is operated since 2005. Largest mixing ratios are found in the troposphere, and reach 1.2 ppbv for C_2H_6, 1 ppbv for HCN, 600 pptv for PAN, and 450 pptv for C_2H_2. The estimated precision in case of significantly enhanced mixing ratios (including measurement noise and propagation of uncertain parameters randomly varying in the time domain) and altitude resolution are typically 10 %, 3–4.5 km for C_2H_6, 15 %, 4–6 km for HCN, 6 %, 2.5–3.5 km for PAN, and 7 %, 2.5–4 km for C_2H_2.

1 Introduction

The MIPAS instrument onboard the ESA's Envisat research satellite (Fischer et al., 2008) measures atmospheric limb emission in the mid-infrared (IR) spectral region in five spectral bands between 685 cm^{-1} and 2410 cm^{-1}. From the spectra retrieval of a high number of atmospheric constituents is possible. From June 2002 to March 2004 MIPAS measured at a spectral resolution of 0.025 cm^{-1} (high spectral resolution, HR). After a failure of the interferometer slide operation resumed in January 2005 at a degraded spectra resolution of 0.0625 cm^{-1} (reduced spectral resolution, RR), however at improved horizontal and vertical sampling. Retrievals of temperature and stratospheric constituents, namely H_2O, O_3, HNO_3, CH_4, N_2O, $ClONO_2$ and ClO from reduced spectral resolution spectra already have been published by von Clarmann et al. (2009b).

In this paper we present RR retrievals of gases which are important in the upper troposphere: C_2H_6, C_2H_2, HCN, and PAN. These retrievals are performed with the IMK-IAA research processor which is one of different MIPAS-Envisat processors.

AMTD
4, 5389–5424, 2011

2 Measurements

The MIPAS instrument measures atmospheric emission in mid-IR in limb geometry from a sunsynchroneous polar orbit at an altitude of about 800 km. All of the measurements described in this paper are performed in the so-called reduced resolution nominal mode with 27 tangent altitudes per limb scan. The scanning pattern varies with latitude; the lowermost nominal tangent altitudes are 6 km close to the poles and 12 km at the equator. The uppermost tangent altitudes vary between 70 and 76 km, respectively. The tangent altitude increment increases with altitude from 1.5 km at the lowermost part of the scan pattern to 4 km at the uppermost altitudes (cf. http://www.atm.ox.ac.uk/group/mipas/rrmodes.html). The along-track sampling is about 400 km. During one day close to 1500 profiles are measured in 15 orbits.

3 Retrieval

The retrieval follows the strategy described in von Clarmann et al. (2003), i.e. radiative transfer calculations are performed with the Karlsruhe Optimized and Precise Radiative Transfer Algorithm (KOPRA, (Stiller et al., 2002)); dedicated spectral regions (so-called "microwindows") are used instead of the entire spectral band in order to gain computational efficiency and to reduce the signal of interfering species (von Clarmann and Echle, 1998; Echle et al., 2000); an empirical continuum emission as well as a zero-level calibration correction is jointly fitted to the spectra to reduce the sensitivity of the retrieval to weakly wavenumber-dependent inaccuracies of radiative transfer modelling and calibration; a regularization scheme based on a Tikhonov-type first order finite differences scheme is used to stabilize the retrieval (Steck and von Clarmann, 2001; Tikhonov, 1963). The used spectroscopic dataset is Hitran04 (Rothman et al., 2005) and corresponding updates (e.g. Allen et al., 2005).

Since the species under assessment do not possess prominent spectral signatures, interference with lines of other species is a major issue. In order to minimize the

AMTD
4, 5389–5424, 2011

propagation of uncertainties in the abundances of interfering species, either vertical profiles resulting from a preceding retrieval of the interferents in a different spectral region are used to model their contribution to the spectral signal (so-called "pre-fit"), or the abundances of the interferents are jointly fitted with the abundances of the target species (so-called "joint-fit") (cf. Table 1). Temperature, tangent altitude information and mixing ratios of the major contributors to the infrared spectrum were taken from von Clarmann et al. (2009b). The retrieval grid has a 1 km spacing up to 44 km and is coarser above (2 km up to 70 km and 5 km up to 120 km). For radiative transfer modelling, a horizontally homogeneous atmosphere in case of trace gas mixing ratios is assumed. However, for temperature, a linear horizontal variation was allowed in a range of 400 km around the nominal geolocation of the limb scan. This improves the accuracy of the retrieval (Kiefer et al., 2010), and in many cases it helps to reduce the number of convergence failures.

3.1 Retrieval of C_2H_6

The retrieval procedure for the MIPAS HR spectra of C_2H_6 was developed by von Clarmann et al. (2007) and Glatthor et al. (2009). The retrievals of C_2H_6 from reduced resolution spectra is performed as described there. Despite the different spectral resolution and tangent altitude grid, their retrieval setup proved robust also for the reduced resolution measurements and required no major modification. The highest tangent altitude used is 52 km. The microwindows used are located between 811.5 cm^{-1} and 835.75 cm^{-1} (cf. Tab. 2).

The regularization chosen leads to the averaging kernels as shown in Fig. 1. While the peak values of the averaging kernels are decreasing with altitude and the averaging kernels are broadened, they are still well-behaved in a sense that they are roughly symmetric and peak at the nominal altitudes. The only awkward feature is the strong negative side wiggle of the 5 km averaging kernel at 10 km.

The altitude resolution, calculated as half width of the rows of the averaging kernel matrix, is about 3 km at lowermost altitudes and degrades to about 9 km at 20 km and

AMTD
4, 5389–5424, 2011

above. Since the altitude resolution of HR measurements remains better than 7 km at higher altitude and reaches similar values in the troposphere, the altitude resolution of RR is a little weaker than that of HR.

The horizontal resolution of the measurement was estimated using the method by von Clarmann et al. (2009a). The horizontal information smearing calculated as the halfwidth of the horizontal component of the 2-D averaging kernel is approximately 410 km at altitudes below 15 km and about 480 km above (see Table 4).

In Fig. 2 the measured and modelled spectrum and the fit residual of both are displayed. In comparison to the residual the spectral contribution of C_2H_6 is shown in the lower part of the plot. The noise eqivalent spectral radiance NESR in the spectral range is about 10.4 nW/(cm^2 sr cm^{-1}) while the root of mean squares RMS of the residual is 29.5 nW/(cm^2 sr cm^{-1}). The part of the residuals not explained by the noise is attributed to parameter uncertainties disscused below but nevertheless the spectral contribution of C_2H_6 exceeds the residual.

The estimated retrieval errors are dominated by measurement noise at the lowermost altitudes (cf. Table 3) and by propagation of ozone uncertainties at altitudes at and above 15 km. The total random (noise plus propagation of random parameter uncertainties) retrieval error is estimated at 76 to 158 pptv for altitudes of 8 to 12 km. This corresponds to a relative error of about 11 % at altitudes up to 12 km for measurements of quite strong mixing ratios, such as in a pollution plume.

3.2 Retrieval of C_2H_2

A method retrieving C_2H_2 from MIPAS HR spectra was developed by Glatthor et al. (2007). Their C_2H_2 is fitted jointly with PAN between 775 cm^{-1} and 800 cm^{-1}. In contrast, we use C_2H_2 emissions in the 730.75 cm^{-1} and 787.8125 cm^{-1} spectral region (see Table 2), and we use prefitted PAN mixing ratios. In our retrieval, ozone is the only jointly fitted species (see Table 1).

AMTD
4, 5389–5424, 2011

The averaging kernels are displayed in Fig. 3. The vertical resolution of RR is better than 4 km below 18 km and worse than 8 km above 24 km and. Negative side wiggles are even more pronounced than those of C_2H_6. The vertical resolution is slightly improved compared to HR at altitudes below 18 km but worse above. The horizontal information smearing is 229 km (see Table 4).

The spectral contribution of C_2H_2 is much higher than that of C_2H_6 (see Fig. 4). While an NESR of 22.2 nW/(cm^2 sr cm^{-1}) is expected and the residual RMS is 46.22 nW/(cm^2 sr cm^{-1}) the contribution of C_2H_2 to the simulated spectrum exceeds the residual by a few times.

The retrieval error of the C_2H_2 retrieval is dominated by noise and tangent altitude uncertainties (see Table 3). The total random retrieval error is estimated at 20 to 30 pptv for altitudes of 8 to 12 km. The total random retrieval error at high mixing ratios is at about 7 %. Again, relative errors are increasing strongly above the altitudes of significant prominence, here at about 13 km.

3.3 Retrieval of HCN

First MIPAS full resolution retrievals of HCN were developed by Glatthor et al. (2007). In contrast to their retrieval setup, here we jointly fit O_3 instead of using pre-fitted O_3 mixing ratios. This leads to a better agreement between measured and modelled radiances and hints at inconsistencies of ozone spectroscopic data in the spectral region used for the HCN retrieval and that used for the regular O_3 retrievals. Since ozone uncertainties are the dominating parameter error source of the HCN retrieval, this additional effort is justified. Further, we use a different set of microwindows, to cope with worse spectral interference problem at the reduced spectral resolution (cf. Table 2). The use of the original microwindow set of the full resolution retrievals would lead to a high bias of HCN at altitudes above 30 km.

The averaging kernels of HCN yield smaller peak values than those of C_2H_6 and thus are wider (Fig. 5) but there is no issue with negative side wiggles. The altitude resolution is about 4 km at lowermost altitudes and degrades to 6 km at 25 km. Above

AMTD
4, 5389–5424, 2011

40 km, it is worse than 10 km. Compared to HCN HR measurements (Glatthor et al., 2007) the altitude resolution at RR is slightly improved. The horizontal information smearing is approximately 425 km at altitudes below 15 km and about 500 km above (see Table 4).

The residual between the measured and the modelled spectrum is plotted in Fig. 6 along with the measured and the modelled spectrum. While NESR is at about 13.4 nW/(cm^2 sr cm^{-1}) the RMS of the residual is at about 40.0 nW/(cm^2 sr cm^{-1}). The spectral contribution of HCN outmatches the residual in most microwindows significantly.

Random parameter errors are the main error source at most altitudes (see Table 3). Depending on altitude, the error budget is dominated by tangent altitude pointing uncertainties, measurement noise, spectral shift, and at a few altitudes interference by N_2O_5. The total random retrieval error is estimated at 95 to 115 pptv for altitudes of 8 to 12 km and at 32 to 54 pptv for altitudes of 15 to 30 km. The relative error is less than 15 % at lowermost altitudes and less than 25 % up to 30 km.

3.4 Retrieval of PAN

The peroxyacetyl nitrate (PAN) retrieval from reduced resolution spectra has been modified with respect to the PAN retrievals developed for full resolution MIPAS spectra by Glatthor et al. (2007). Like for HCN retrievals, O_3 is now jointly retrieved instead of being prefitted. The microwindows have been adjusted slightly to the reduced resolution spectra (cf. Table 2). Small microwindows in the 775 cm^{-1}–800.0 cm^{-1} spectral region were merged. This led to a better determined retrieval of the background continuum since in our retrieval the jointly fitted background continuum assigns one continuum variable per microwindow. However, the gap between 790.5 cm^{-1} and 794.5 cm^{-1} has been kept in order to avoid interference problems with the CO_2 Q-branch at 792 cm^{-1}.

The altitude resolution of the retrievals which is about 2.5 km at lowermost altitudes, degrades to 4 km at 15 km, and more than 7 km at 25 km and above (cf. Fig. 7). The altitude resolution of HR PAN retrievals is comparable but does not go below 4 km. The

AMTD
4, 5389–5424, 2011

horizontal information smearing is approximatly 315 km at altitudes below 15 km and about 495 km above (see Table 4).

Figure 8 exibits the spectra, the spectral residual and the contribution of PAN at a single retrieval. The expected NESR is about 10.8 nW/(cm^2 sr cm^{-1}) and the RMS of the residual is about 26.9 nW/(cm^2 sr cm^{-1}). The contribution of PAN exceeds the RMS clearly.

Dominating error sources are measurement noise and tangent altitude pointing uncertainty (Table 3). The total random retrieval error is estimated at 27 to 45 pptv for altitudes of 8 to 12 km. The total relative error in lowermost altitudes is about 7 % and less.

4 Results

In the following, we show selected examples of measurements in October 2007. This period has been selected because of the plumes which are formed by biomass burning regularly at October in southern midlatitudes (Singh et al., 1996; Glatthor et al., 2009). Single orbit volume mixing ratios (vmr) as well as monthly mean vmrs will be shown.

4.1 C_2H_6

Ethane (C_2H_6) is the most important non-methane hydrocarbon (Singh et al., 2001) in the troposphere. Its sources are supposed to be anthropogenically or production by biomass burning. While most recent papers (e.g. Xiao et al., 2008) estimate industrial activity as dominating, former ones (Rudolph, 1995) propose equality between both sources. Dominating sinks are reaction with OH in the troposphere and with atomic chlorine (Cl) in the stratosphere (Aikin et al., 1982).

Mixing ratios of C_2H_6 measured by MIPAS close to the tropopause often reach values of 400 pptv and up to 1.2 ppbv at highly polluted air masses at single measurements. In Fig. 9 such an air mass can be found at about 30° South when the satellite passes

AMTD
4, 5389–5424, 2011

this latitude for the first time at the shown orbit. For HR measurements (Glatthor et al., 2009) mixing ratios up to 700 pptv at single locations were found.

We observed the maximium monthly mean mixing ratios of C_2H_6 in October 2007 at about 800 pptv. For monthly means of the same month in different years the RR mixing ratios fit well to the HR mixing ratios. In October 2003 Glatthor et al. (2009) found mixing ratios of about 600 pptv close to Africa, while RR measurements in October 2007 show mixing ratios of about 800 pptv above the southern Atlantic Ocean at most similar latitudes (Fig. 10). In addition, mean HR mixing ratios of C_2H_6 for another time period close to October 2003 (von Clarmann et al., 2007) show comparable mixing ratios as well (approx. 600 pptv) with maximum values at a biomass burning plume location.

Outside of the tropics in lower altitudes and thus below tropopause as well, less prominent but nevertheless significant enhancements of C_2H_6 can be found at northern latitudes especially above Asia (Fig. 10). These generally higher values in the northern hemisphere may be attributed to antropogenic activities.

4.2 C_2H_2

The sources and sinks of ethine (C_2H_2) are similar to those of ethane, although the relative importance of biomass burning is larger (Singh et al., 1996).

Similar as the pollutants discussed before, MIPAS measurements of C_2H_2 show significantly increased mixing ratios at 30° S at the orbit plotted in Fig. 11. Mixing ratios up to 400 pptv are reached there, while few other measurements reach about 100 pptv and most of them are close to zero. Glatthor et al. (2007) found mixing ratios of C_2H_2 at single MIPAS HR measurements performed in October until December 2003 of up to 400 pptv as well.

The monthly mean mixing ratios reveal a global background of about 40 pptv or 50 pptv while maximum values reach up to 200 pptv in October 2007 in 12 km above the southern Altantic Ocean, and some other regions as well (See Fig. 12). Monthly means of MIPAS HR C_2H_2 retrievals for August 2003 in 200 hPa retrieved by Parker

AMTD
4, 5389–5424, 2011

et al. (2010) show peak (approx. 200 pptv) and background (approx. 50 pptv) mixing ratios very close to our MIPAS RR monthly mean mixing ratios.

Singh et al. (1996) measured median mixing ratios in polluted air masses by in situ measurements above the southern Atlantic Ocean of 160 pptv and 50 pptv as background at 11.5 km in September and October 1992.

4.3 HCN

HCN is well mixed in the troposphere and has slowly decreasing mixing ratios due to loss by reaction with OH and O(1D) in the stratosphere (Cicerone and Zellner, 1983). Spaceborne measurements (Rinsland et al., 1998) led to the conclusion that HCN mainly is produced by biomass burning and may be utilised as a tracer for such events (Singh et al., 2001; Li et al., 2003; Glatthor et al., 2007).

Mixing ratios of HCN at the sample orbit (Fig. 13) exhibit mixing ratios of about 200 pptv at lowermost altitudes close to tropopause throughout all latitudes. Polluted air masses show mixing ratios up to 1 ppbv. Glatthor et al. (2009) obtained mixing ratios of about 300 pptv by HR single measurements at all latidues and longitudes at 12 km altitude. HR peak values reach 500 pptv. ATMOS measurements (Rinsland et al., 1998) reveal mixing ratios close to 1 ppbv at one measurement and above 400 pptv for a few others at comparable altitudes while background values are between 200 and 300 pptv.

While the HR measurements performed by Glatthor et al. (2009) for October 2003 reach monthly means of 500 pptv, the RR mixing ratios exceed 600 pptv above the southern Atlantic Ocean in October 2007 at 12 km (Fig. 14) at the same altitude. Regional enhancements of HCN polewards of 40° at 8 km are found in both hemispheres. They are presumed to be advected from biomass burning event at lower latitudes or boreal fires.

AMTD
4, 5389–5424, 2011

4.4 PAN

Peroxyacetyl nitrate (PAN) is produced from tropospheric precursors. The precursors are hydrocarbons which have been transformed at different steps to a peroxyacetyl radical $CH_3C(O)OO$. A reversible reaction of the peroxyacetyl radical with nitrate (NO_2) leads to PAN. The lifetime of PAN is strongly temperature dependent (Singh, 1987) with up to 5 months at 250 K and about an hour at 298 K. Thus the lifetime at the tropopause level exceeds the lifetime in lower troposphere and upper stratosphere.

Peak mixing ratios of PAN measured by MIPAS at reduced spectral resolution reach more than 500 pptv (Fig. 15). At several other locations mixing ratios up to 250 pptv are obtained. The RR monthly mean measurements show background values of about 100 pptv except of northern midlatitudes and northwards (Fig. 16). There, more than 200 pptv are reached at most locations. At polluted areas, e.g. the southern Atlantic Ocean at 12 km, PAN mixing ratios exceed 400 pptv.

Upper tropospheric ten-day mean PAN mixing ratios in October 2003, which falls in the MIPAS HR period, reach 500 pptv (Glatthor et al., 2007); their tropospheric background mixing ratios were below 100 pptv at southern latitudes and about 150 pptv at northern latitudes. Further MIPAS HR retrievals were performed by Moore and Remedios (2010). These authors found similar backgrounds at global monthly means in January 2003. Their peak values are close to 500 pptv at 300 hPa and about 225 pptv at 201 hPa. These HR results are in good agreement to our PAN results retrieved from MIPAS RR spectra.

Furthermore, Singh et al. (1996) measured in situ at 12 km of altitude median mixing ratios of about 100 pptv as backround and above 300 pptv at polluted air masses in September and October 1992.

AMTD
4, 5389–5424, 2011

5 Conclusions

MIPAS onboard Envisat is able to measure pollutants in the upper troposphere also at reduced spectral resolution which is applied since beginning of 2005. HCN, PAN, and C_2H_2 can be measured with a slightly better altitude resolution compared to the high spectral resolution mode at most levels. Only the C_2H_6 measurements have a reduced altitude resolution. The improvements refer particularly to the upper troposphere.

In case of significantly enhanced mixing ratios, like in biomass burning plumes, the total relative random errors of all species under assessment are 15 % or below. Plumes of different compositions and different mixing ratio enhancements can be found.

The retrieved mixing ratios at reduced spectral resolution are in good agreement with the mixing ratios obtained by high resolution measurements or measured by other instruments. No indication for inconsistency between the different measurements has been detected. Comparison with results found in literature suggests that the chemical charakteristics of biomass burning plumes with respect to C_2H_6, C_2H_2, HCN, and PAN have been quite similar in the time periods analyzed.

Acknowledgements. The work was funded by DFG under contract number GL 643/1-1, project POMODORO. ESA has provided MIPAS level-1. The retrievals of IMK/IAA were performed on the HP XC4000 of the Scientific Supercomputing Center (SSC) Karlsruhe under project grant MIPAS. IMK data analysis was supported by DLR under contract number 50EE0901.

References

Aikin, A. C., Herman, J. R., Maier, E. J., and McQuillan, C. J.: Atmospheric Chemistry of Ethane and Ethylene, J. Geophys. Res., 87(C4), 3105–3118, 1982. 5396

Allen, G., Remedios, J. J., Newnham, D. A., Smith, K. M., and Monks, P. S.: Improved mid-infrared cross-sections for peroxyacetyl nitrate (PAN) vapour, Atmos. Chem. Phys., 5, 47–56, doi:10.5194/acp-5-47-2005, 2005. 5391

Chatfield, R. B., Vastano, J. A., Li, L., Sachse, G. W., and Connors, V. S.: The Great African

AMTD
4, 5389–5424, 2011

plume from biomass burning, in : Generalizations from a three-dimensional study of TRACE A carbon monoxide, J. Geophys. Res., 103, 28059–28077, 1998.
Cicerone, R. J. and Zellner, R.: The Atmospheric Chemistry of Hydrogen Cyanide (HCN), J. Geophys. Res., 88(C15), 10689–10696, 1983. 5398
Echle, G., von Clarmann, T., Dudhia, A., Flaud, J.-M., Funke, B., Glatthor, N., Kerridge, B., López-Puertas, M., Martín-Torres, F. J., and Stiller, G. P.: Optimized spectral microwindows for data analysis of the Michelson Interferometer for Passive Atmospheric Sounding on the Environmental Satellite, Appl. Optics, 39, 5531–5540, 2000. 5391
Fischer, H., Birk, M., Blom, C., Carli, B., Carlotti, M., von Clarmann, T., Delbouille, L., Dudhia, A., Ehhalt, D., Endemann, M., Flaud, J. M., Gessner, R., Kleinert, A., Koopman, R., Langen, J., López-Puertas, M., Mosner, P., Nett, H., Oelhaf, H., Perron, G., Remedios, J., Ridolfi, M., Stiller, G., and Zander, R.: MIPAS: an instrument for atmospheric and climate research, Atmos. Chem. Phys., 8, 2151–2188, doi:10.5194/acp-8-2151-2008, 2008. 5390
Glatthor, N., von Clarmann, T., Fischer, H., Funke, B., Grabowski, U., Höpfner, M., Kellmann, S., Linden, A., Milz, M., Steck, S., and Stiller, G.: Global peroxyacetyl nitrate (PAN) retrieval in the upper troposphere from limb emission spectra of the Michelson Interferometer for Passive Atmospheric Sounding (MIPAS), Atmos. Chem. Phys., 7, 2775–2787, doi:10.5194/acp-7-2775-2007, 2007. 5393, 5394, 5395, 5397, 5398, 5399
Glatthor, N., von von Clarmann, T., Stiller, G., Funke, B., Koukouli, M. E., Fischer, H., Grabowski, U., Höpfner, M., Kellmann, S., and Linden, A.: Large-scale upper tropospheric pollution observed by MIPAS HCN and C_2H_6 global distributions, Atmos. Chem. Phys., 9, 9619–9634, doi:10.5194/acp-9-9619-2009, 2009. 5392, 5396, 5397, 5398
Kiefer, M., Arnone, E., Dudhia, A., Carlotti, M., Castelli, E., von Clarmann, T., Dinelli, B. M., Kleinert, A., Linden, A., Milz, M., Papandrea, E., and Stiller, G.: Impact of temperature field inhomogeneities on the retrieval of atmospheric species from MIPAS IR limb emission spectra, Atmos. Meas. Tech., 3, 1487–1507, doi:10.5194/amt-3-1487-2010, 2010. 5392
Li, Q., Jacob, D. J., Yantosca, R. M., Heald, C. L., Singh, H. B., Koike, M., Zhao, Y., Sachse, G. W., and Streets, D. G.: A global three-dimensional model analysis of the atmospheric budgets of HCN and CH_3CN: Constraints from aircraft and ground measurements, J. Geophys. Res., 108(D21), 8827, doi:10.1029/2002JD003075, 2003. 5398
Moore, D. P. and Remedios, J. J.: Seasonality of Peroxyacetyl nitrate (PAN) in the upper troposphere and lower stratosphere using the MIPAS-E instrument, Atmos. Chem. Phys., 10, 6117–6128, doi:10.5194/acp-10-6117-2010, 2010. 5399

AMTD
4, 5389–5424, 2011

Parker, R. J., Remedios, J. J., Moore, D. P., and Kanawade, V. P.: Acetylene C2H2 retrievals from MIPAS data and regions of enhanced upper tropospheric concentrations in August 2003, Atmos. Chem. Phys. Discuss., 10, 29735–29771, doi:10.5194/acpd-10-29735-2010, 2010. 5397

Rinsland, C. P., Gunson, M. R., Wang, P.-H., Arduini, R. F., Baum, B. A., Minnis, P., Goldman, A., Abrams, M. C., Zander, R., Mahieu, E., Salawitch, R. J., Michelsen, H. A., Irion, F. W., and Newchurch, M. J.: ATMOS/ATLAS 3 Infrared Measurements of Trace Gases in the November 1994 Tropical and Subtropical Upper Troposphere, J. Quant. Spectrosc. Ra., 60(5), 891–901, 1998. 5398

Rothman, L. S., Jacquemart, D., Barbe, A., Chris Benner, D., Birk, M., Brown, L. R., Carleer, M. R., Chackerian, Jr., C., Chance, K., Coudert, L. H., Dana, V., Devi, V. M., Flaud, J.-M., Gamache, R. R., Goldman, A., Hartmann, J.-M., Jucks, K. W., Maki, A. G., Mandin, J.-Y., Massie, S. T., Orphal, J., Perrin, A., Rinsland, C. P., Smith, M. A. H., Tennyson, J., Tolchenov, R. N., Toth, R. A., Vander Auwera, J., Varanasi, P., and Wagner, G.: The HITRAN 2004 molecular spectroscopic database, J. Quant. Spectrosc. Ra., 96, 139–204, doi:10.1016/j.jqsrt.2004.10.008, 2005. 5391

Rudolph, J.: The tropospheric distribution and budget of ethane, J. Geophys. Res., 100(D6), 11369–11381, 1995. 5396

Singh, H.: Reactive nitrogen in the troposphere, Environ. Sci. Technol., 21(4), 320–327, 1987. 5399

Singh, H. B., Herlth, D., Kolyer, R., Chatfield, R., Viezee,W., Salas, L. J., Chen, Y., Bradshaw, J. D., Sandholm, S. T., Talbot, R., Gregory, G. L., Anderson, B., Sachse, G. W., Browell, E., Bachmeier, A. S., Blake, D. R., Heikes, B., Jacob, D., and H. E. Fuelberg: Impact of biomass burning emissions on the composition of the South Atlantic troposphere: Reactive nitrogen and ozone, J. Geophys. Res., 101(D19), 24203–24219, 1996. 5396, 5397, 5398, 5399

Singh, H., Chen, Y., Staudt, A., Jacob, D., Blake, D., Heikes, B., and Snow, J.: Evidence from the Pacific troposphere for large global sources of oxygenated organic compounds, Nature, 410, 1078, doi:10.1038/35074067, 2001. 5396, 5398

Steck, T., and von Clarmann, T.: Constrained Profile Retrieval Applied to the Observation Mode of the Michelson Interferometer for Passive Atmospheric Sounding, Appl. Opt., 40, 3559–3571, 2001. 5391

Stiller, G. P., von Clarmann, T., Funke, B., Glatthor, N., Hase, F., Höpfner, M., and Linden, A.: Sensitivity of trace gas abundances retrievals from infrared limb emission spectra to

AMTD
4, 5389–5424, 2011

simplifying approximations in radiative transfer modelling, J. Quant. Radiat. Transfer, 72(3), 249–280, 2002. 5391

Tikhonov, A.: On the solution of incorrectly stated problems and method of regularization, Dokl. Akad. Nauk. SSSR, 151, 501–504, 1963. 5391

von Clarmann, T., and Echle, G.:Selection of Optimized Microwindows for Atmospheric Spectroscopy, Appl. Opt., 37, 7661-7669, 1998. 5391

von Clarmann, T., Glatthor, N., Grabowski, U., Höpfner, M., Kellmann, S., Kiefer, M., Linden, A., Mengistu Tsidu, G., Milz, M., Steck, T., Stiller, G. P., Wang, D. Y., Fischer, H., Funke, B., Gil-López, S., and López-Puertas, M.: Retrieval of temperature and tangent altitude pointing from limb emission spectra recorded from space by the Michelson Interferometer for Passive Atmospheric Sounding (MIPAS), J. Geophys. Res., 108, 4736, doi:10.1029/2003JD003602, 2003. 5391

von Clarmann, T., Glatthor, N., M.E., Koukouli, M.E., Stiller, G., Funke, B., Grabowski, U., Höpfner, M., Kellmann, S., Linden, A., Milz, M., Steck, T., and Fischer, H.: MIPAS measurements of upper tropospheric C_2H_6 and O_3 during the southern hemispheric biomass burning season in 2003, Atmos. Chem. Phys., 7, 5861–5872, doi:10.5194/acp-7-5861-2007, 2007. 5392, 5397

von Clarmann, T., De Clercq, C., Ridolfi, M., Höpfner, M., and Lambert, J.-C.: The horizontal resolution of MIPAS, Atmos. Meas. Tech., 2, 47–54, doi:10.5194/amt-2-47-2009, 2009 5393, 5408

von Clarmann, T., Höpfner, M., Kellmann, S., Linden, A., Chauhan, S., Funke, B., Grabowski, U., Glatthor, N., Kiefer, M., Schieferdecker, T., Stiller, G. P., and Versick, S.: Retrieval of temperature, H_2O, O_3, HNO_3, CH_4, N_2O, $ClONO_2$ and ClO from MIPAS reduced resolution nominal mode limb emission measurements, Atmos. Meas. Tech., 2, 159–175, doi:10.5194/amt-2-159-2009, 2009. 5390, 5392

Xiao, Y., Logan, J. A., Jacob, D. J., Hudman, R. C., Yantosca, R., and Blake, D. R.: Global budget of ethane and regional constraints on US sources, J. Geophys. Res., 113, D21306, doi:10.1029/2007JD009415, 2008. 5396

AMTD
4, 5389–5424, 2011

Table 1. Prefitted (*P*) and jointly fitted (*J*) parameters. Spectral shift, temperature, line-of-sight and HNO_3 are prefits at all retrievals.

species	C_2H_6	HCN	PAN	C_2H_2
H_2O	*P*	*P*	*J*	*P*
O_3	*P*	*J*	*J*	*J*
CH_4	*P*			*P*
N_2O		*P*		*P*
$ClONO_2$	*P*	*P*	*J*	*P*
ClO	*P*	*P*	*P*	
N_2O_5		*P*		*P*
HNO_4	*P*	*P*		
CFC−11	*P*		*P*	
CFC−12	*P*			
NO_2		*P*		
C_2H_6		*P*	*P*	
PAN				*P*
HCN			*P*	
CFC−22			*J*	
C_2H_2			*J*	
CH_3CCl_3			*J*	
CCl_4			*J*	

AMTD
4, 5389–5424, 2011

Table 2. Microwindows and upper altitude limits (in brackets) for MIPAS reduced resolution nominal mode retrievals (cm^{-1}).

C_2H_6* (52 km)	HCN* (68 km)	C_2H_2* (35 km)
811.5000–811.8750	715.5000–718.0000	730.7500–731.3125
814.1875–814.5000	732.4375–735.8125	738.4375–738.7500
816.8750–817.1250	737.5000–741.6250	743.1250–743.5625
819.3750–819.8125	744.3125–747.8125	750.1875–750.4375
822.1875–822.5000	750.1875–753.8750	755.1250–759.8750
824.5000–825.1250	756.0000–760.7500	762.0000–767.0625
827.3750–827.7500	767.8125–770.9375	767.1250–772.1250
829.9375–830.4375	773.6250–776.8125	773.5625–778.5000
831.4375–831.7500	779.3750–782.7500	782.8750–787.8125
832.6250–833.1250		789.8750–790.1250
833.9375–834.2500		799.1250–799.4375
835.5000–835.7500		1309.3750–1311.7500
		1316.1875–1316.3750
PAN (33 km)		
775.000–787.0000		
794.500–800.0000		

* Not all spectral gridpoints are used at each altitude, depending on interference by other species.

AMTD
4, 5389–5424, 2011

Table 3. Total errors of the retrievals in pptv and percent and the five most contributing error sources (pptv); LOS = Line Of Sight; ILS = Instrumental Line Shape. The errors are calculated for a single biomass burning plume location with enhanced mixing ratios of all gases.

C_2H_6	8 km	10 km	12 km	15 km	20 km
total	160	140	82	170	140
total (%)	11.2	10.6	8.9	82.6	>>100
noise	150	130	71	70	61
LOS	51	48	33	0.8	0.2
PAN	35	32	13	6	1.2
gain	6.9	6.1	0.2	13	24
O_3	5.7	4.8	18	150	130
C_2H_2	8 km	10 km	12 km	15 km	20 km
total	30	27	20	9.5	9.5
total (%)	7.1	6.8	6.8	54.1	>100
noise	23	20	8.5	8.9	6.6
LOS	18	18	18	1.8	2.1
PAN	4.8	4.2	4.2	0.7	0.1
ILS	4.4	4.0	2.3	0.7	1.6
gain	3.9	3.7	1.4	0.8	1.3

AMTD
4, 5389–5424, 2011

Fig. 3. Continued.

HCN	8 km	12 km	16 km	20 km	30 km	40 km
total	120	96	35	32	54	76
total (%)	13.0	11.9	14.4	17.9	21.7	68.2
noise	43	36	23	25	32	42
LOS	100	83	14	5.5	3.6	7.9
gain	23	16	0.8	7.0	7.8	3.2
T	21	16	0.6	1	5.4	4.9
ILS	13	12	11	7.3	10	7.5

PAN	8 km	10 km	12 km	15 km	20 km
total	45	31	27	19	18
total(%)	6.9	5.2	5.7	>100	>>100
noise	36	30	16	17	15
LOS	24	5.6	21	7.4	5.1
gain	6.3	1.8	2.7	1.6	4.5
ILS	5.4	2.8	1.9	0.8	0.2
HNO_3	1.7	1.4	0.8	3.5	4.3

AMTD
4, 5389–5424, 2011

Fig. 4. Horizontal averaging kernels (full width at half maximum) calculated according to von Clarmann et al. (2009a).

altitude	7 km	12 km	20 km	34 km	50 km
C_2H_6	416 km	403 km	480 km	485 km	–
C_2H_2	229 km	229 km	229 km	229 km	–
HCN	438 km	417 km	487 km	497 km	494 km
PAN	307 km	327 km	473 km	513 km	–

AMTD
4, 5389–5424, 2011

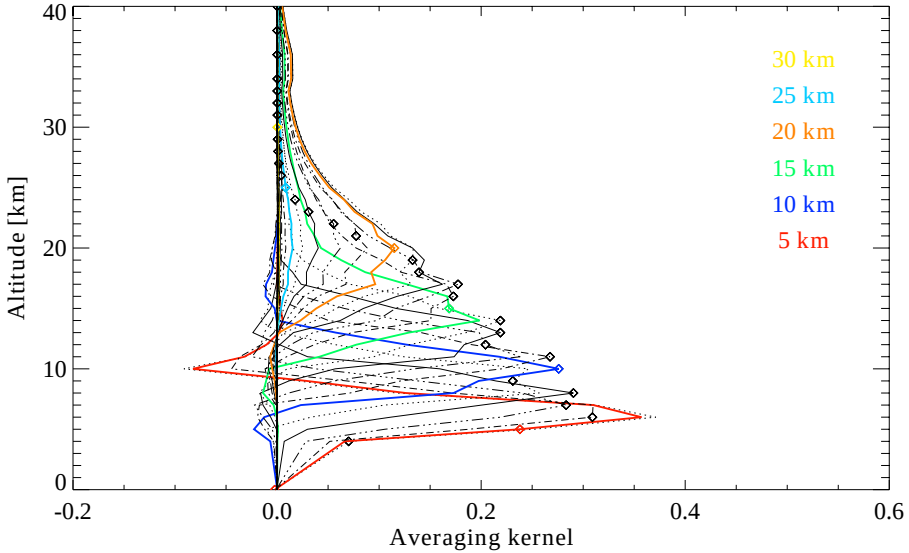

Fig. 1. Rows of the averaging kernel matrix for C_2H_6, evaluated for a limb scan recorded at 80° S, 162° E on 10 October 2009. Selected nominal altitudes are highlighted by colours.

AMTD
4, 5389–5424, 2011

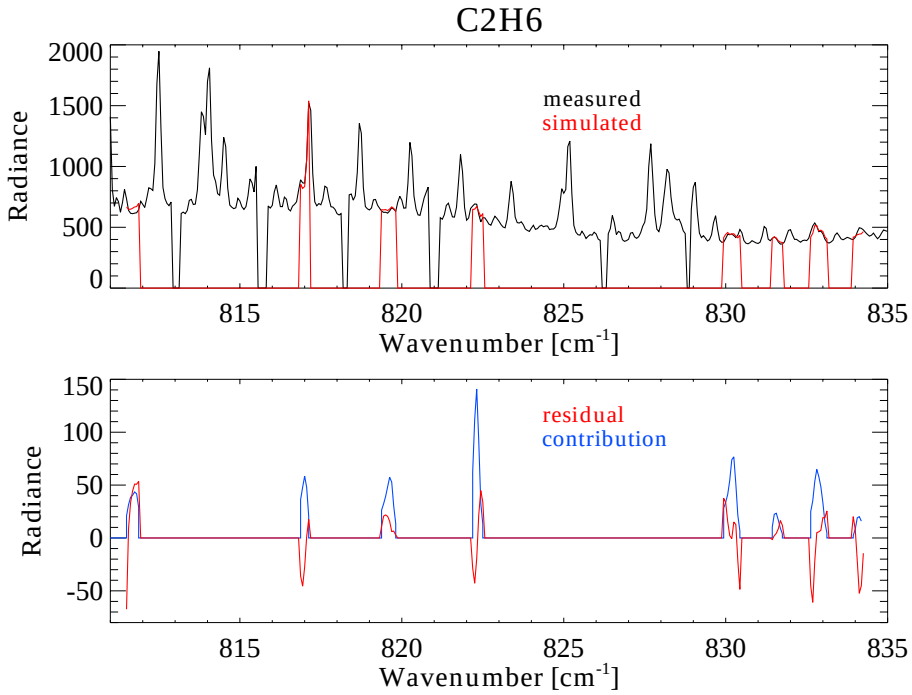

Fig. 2. Measured (black) and simulated (red) spectrum of a single C_2H_6 measurement (upper panel) at 11.0 km. The difference between both is the residual (red) and is plotted in the lower panel. The spectral contribution of C_2H_6 (blue) is calculated as difference between a forward simulation of the atmosphere taking into account all contributing gases and the corresponding forward simulation excluding C_2H_6. Radiances are given in nW/(cm^2 sr cm^{-1}). Gaps in both spectra reflect data points excluded from the analysis.

AMTD
4, 5389–5424, 2011

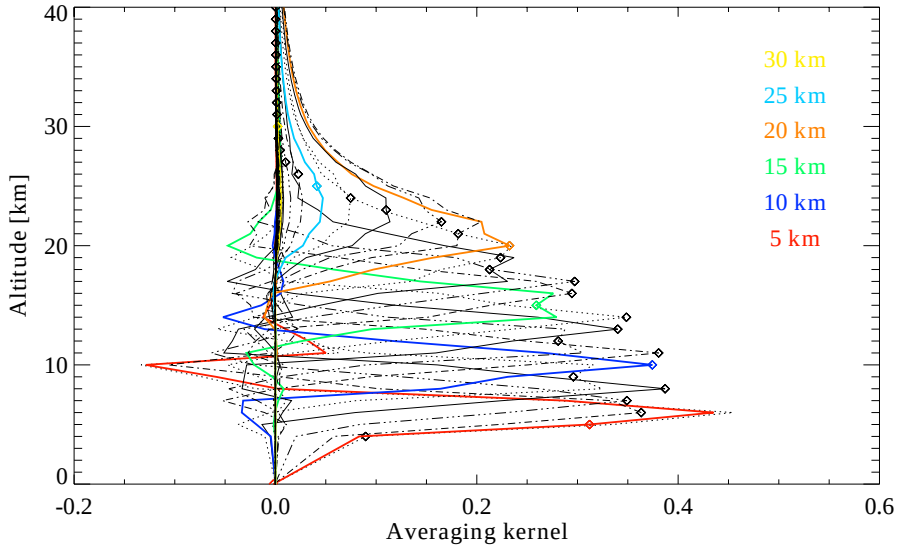

Fig. 3. As Fig. 1 but for C_2H_2.

AMTD
4, 5389–5424, 2011

Global distributions of hydrocarbons from MIPAS RR measurements

A. Wiegele et al.

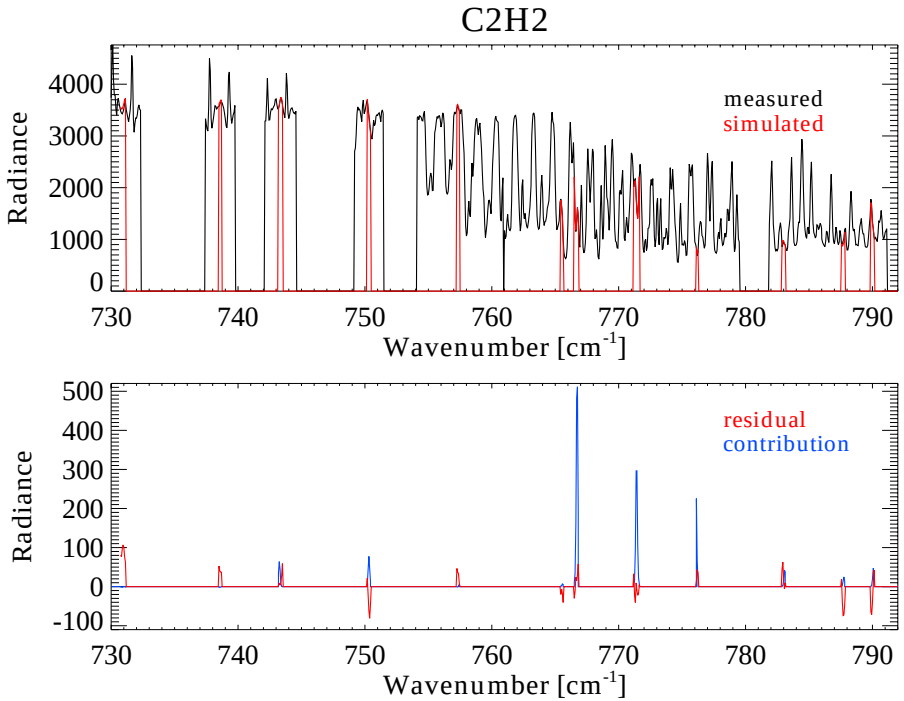

Fig. 4. As Fig. 2 but for C_2H_2.

AMTD
4, 5389–5424, 2011

Global distributions of hydrocarbons from MIPAS RR measurements

A. Wiegele et al.

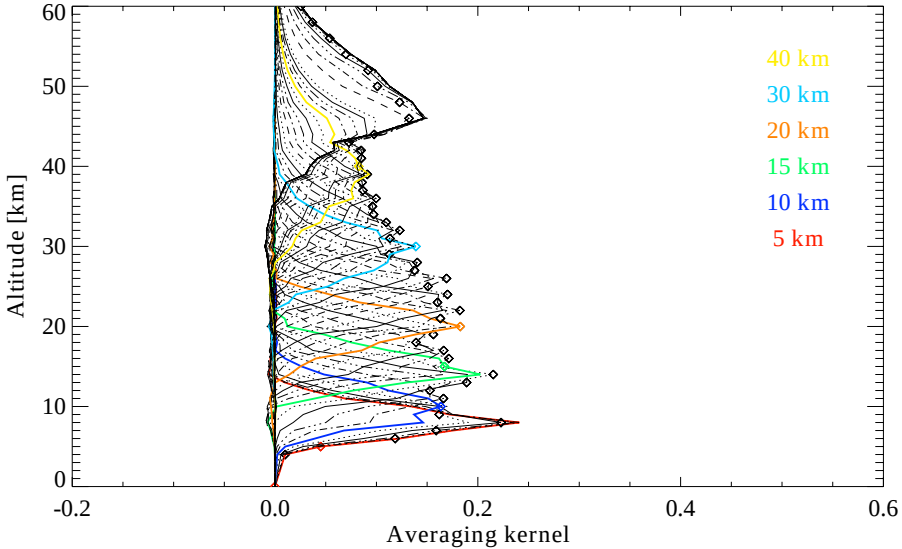

Fig. 5. As Fig. 1 but for HCN.

AMTD
4, 5389–5424, 2011

Global distributions of hydrocarbons from MIPAS RR measurements

A. Wiegele et al.

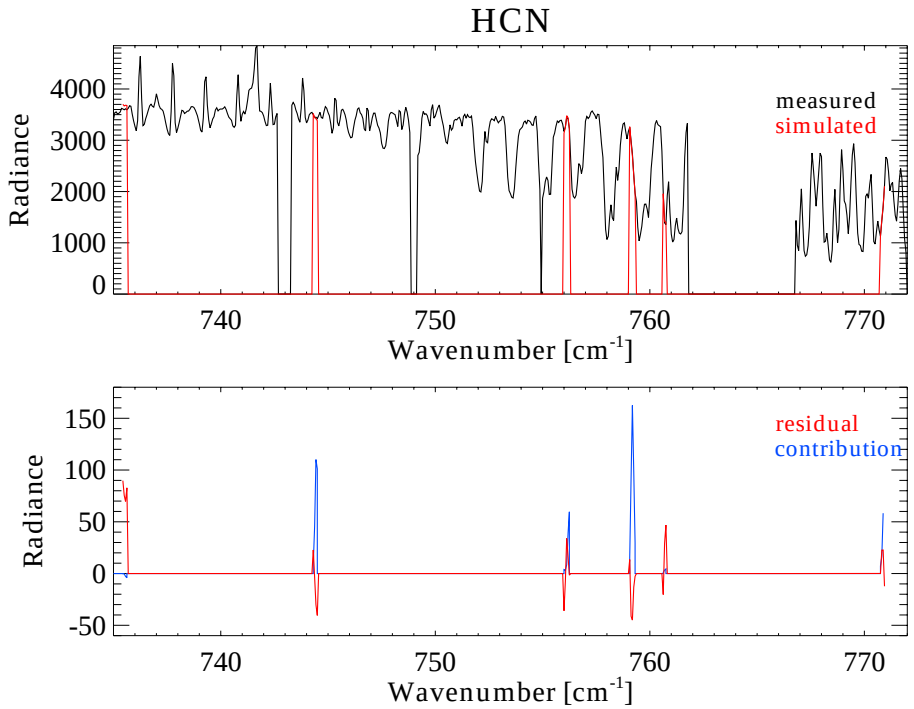

Fig. 6. As Fig. 2 but for HCN.

AMTD
4, 5389–5424, 2011

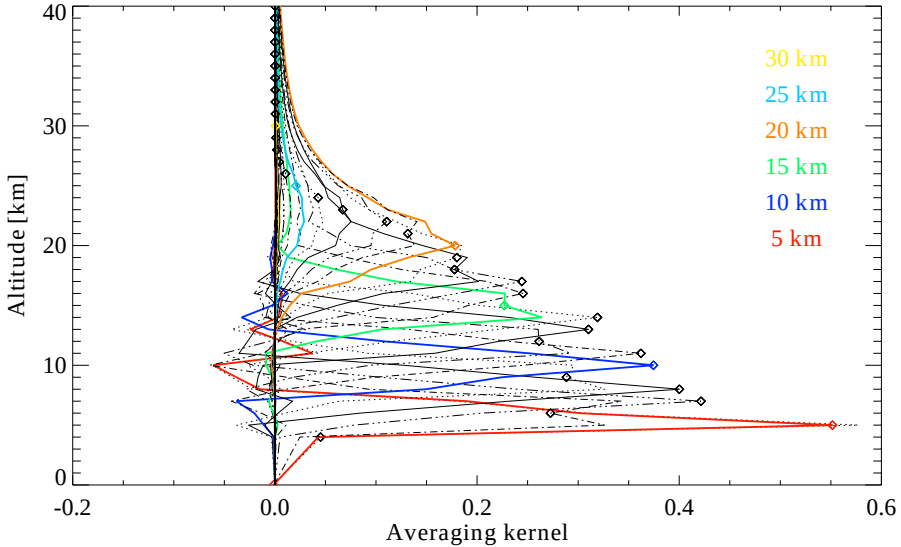

Fig. 7. As Fig. 1 but for PAN.

AMTD
4, 5389–5424, 2011

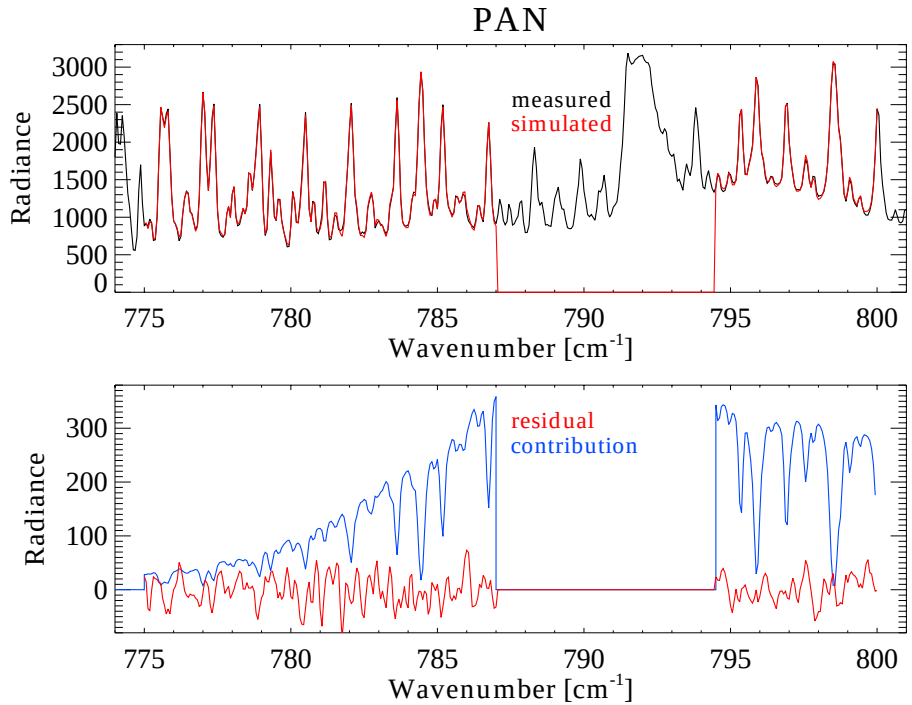

Fig. 8. As Fig. 2 but for PAN.

AMTD
4, 5389–5424, 2011

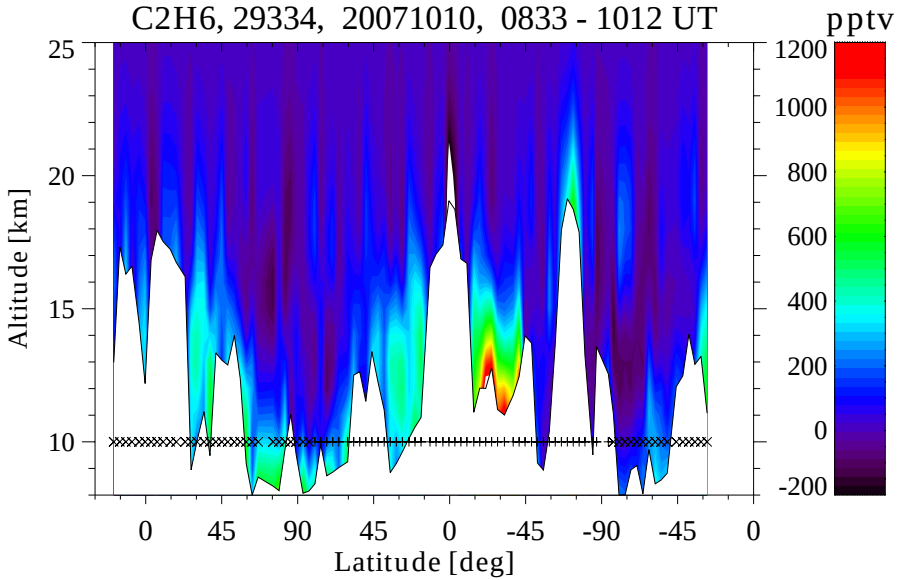

Fig. 9. Single orbit measurements of C_2H_6 vmr. Mixing ratios are plotted versus altitude and latitude.

AMTD
4, 5389–5424, 2011

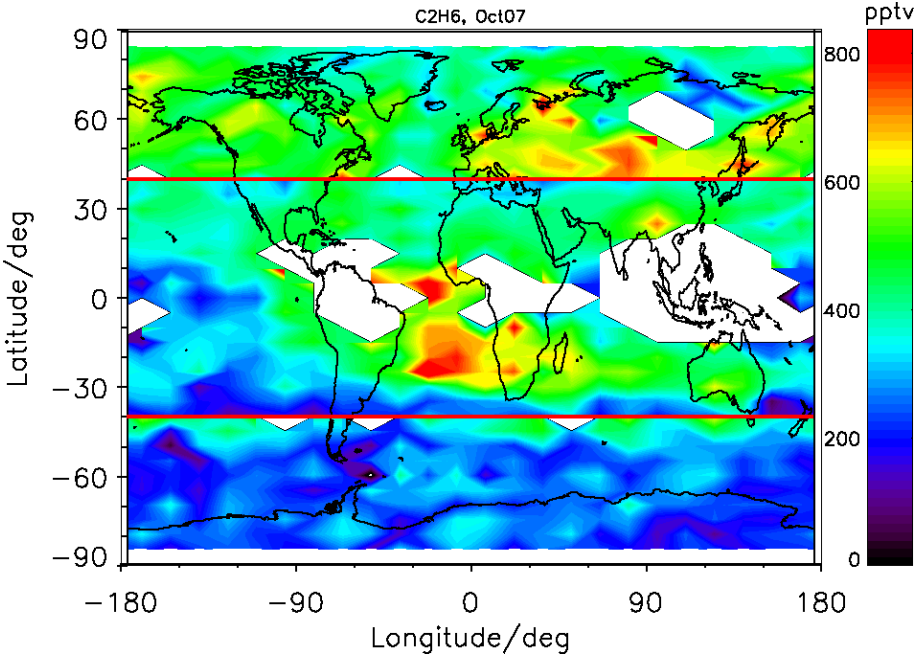

Fig. 10. Global monthly means of C_2H_6 vmr for October 2007. Between the red lines (40° N and S) C_2H_6 vmr is shown at 12 km, at latitudes poleward of 40° at 8 km. This display is choosen to represent the upper troposphere at all latitudes.

AMTD
4, 5389–5424, 2011

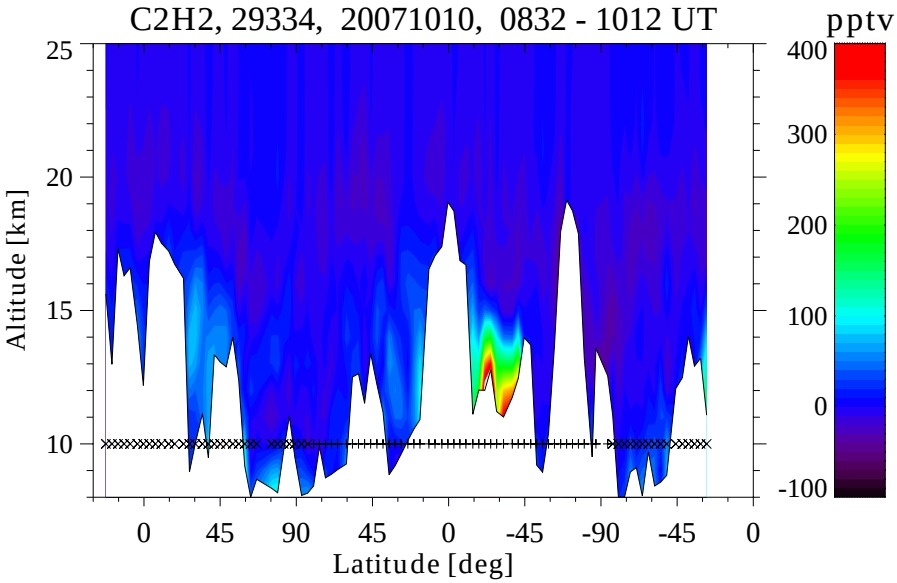

Fig. 11. As Fig. 9 but for C_2H_2.

AMTD
4, 5389–5424, 2011

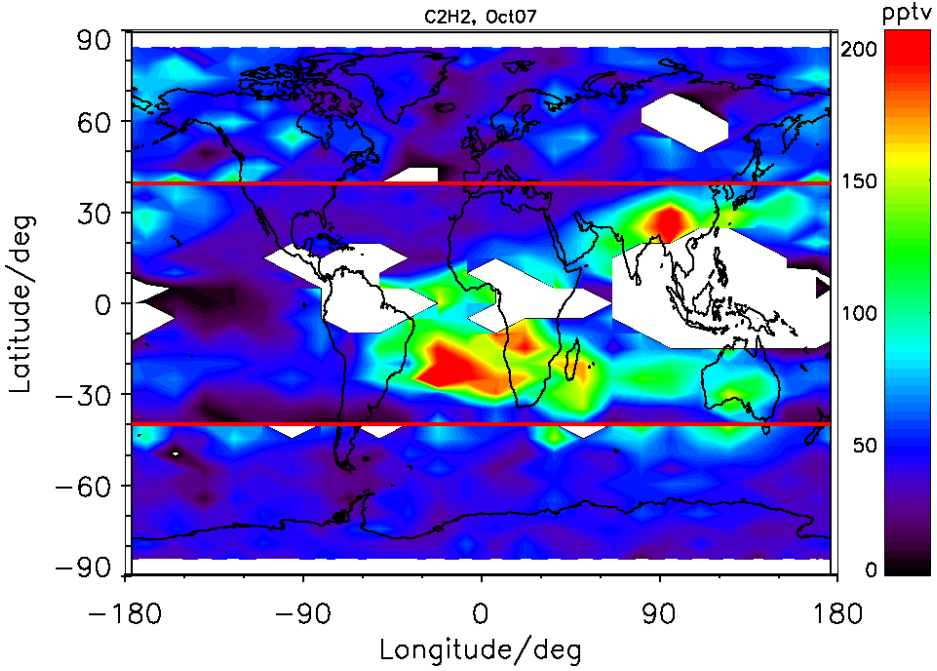

Fig. 12. As Fig. 10 but for C_2H_2.

AMTD
4, 5389–5424, 2011

Global distributions of hydrocarbons from MIPAS RR measurements

A. Wiegele et al.

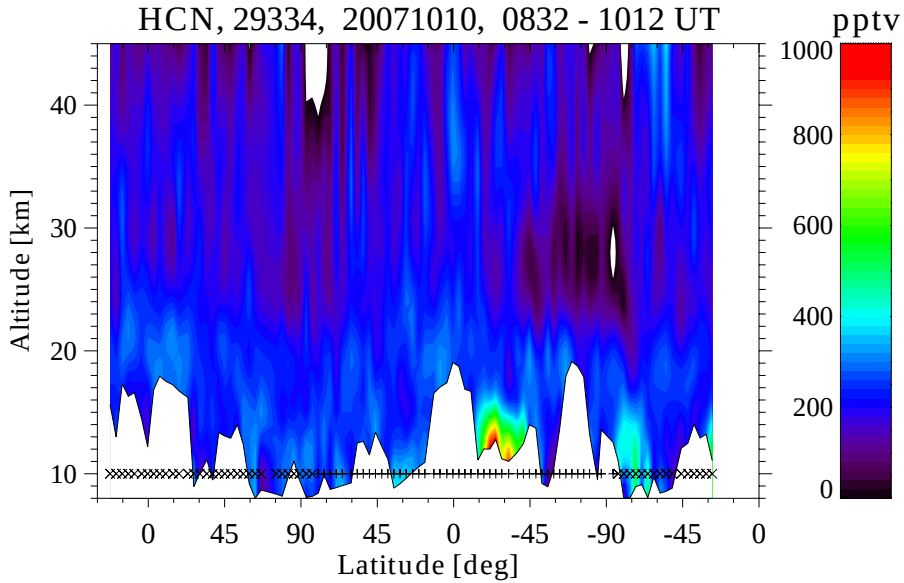

Fig. 13. As Fig. 9 but for HCN.

AMTD
4, 5389–5424, 2011

Global distributions of hydrocarbons from MIPAS RR measurements

A. Wiegele et al.

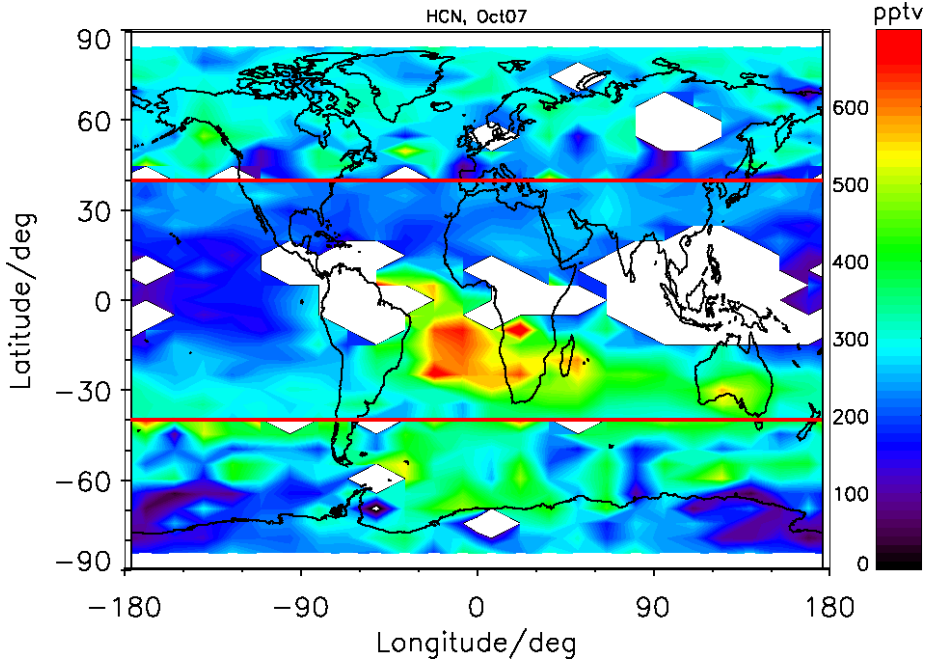

Fig. 14. As Fig. 10 but for HCN.

AMTD
4, 5389–5424, 2011

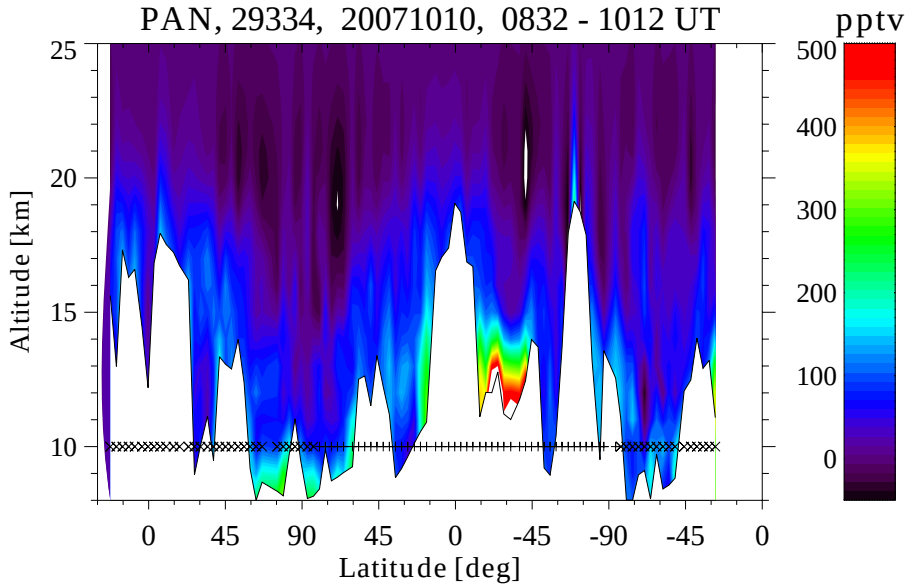

Fig. 15. As Fig. 9 but for PAN.

AMTD
4, 5389–5424, 2011

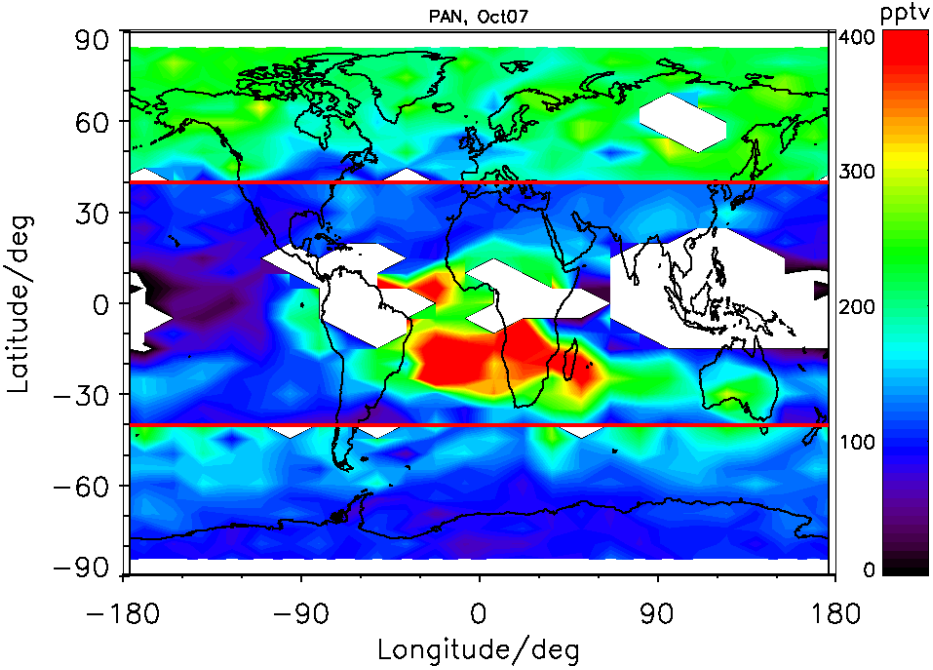

Fig. 16. As Fig. 10 but for PAN.

AMTD
4, 5389–5424, 2011

Global distributions of hydrocarbons from MIPAS RR measurements

A. Wiegele et al.